ACS APPLIED MATERIALS & INTERFACES

Research Article

www.acsami.org

Preparation of Multifunctional Polysaccharide Microcontainers for Lipophilic Bioactive Agents

Tatiana N. Borodina,*[,†] Dmitry O. Grigoriev,[‡] Maria A. Carillo,[‡] Jürgen Hartmann,[‡] Helmuth Moehwald,[‡] and Dmitry G. Shchukin[§]

[†]Laboratory of Bioorganic Structures, Shubnikov Institute of Crystallography Russian Academy of Sciences, Moscow, Russia

[‡]Max Planck Institute of Colloids and Interfaces, Potsdam-Golm, Germany

[§]Stephenson Institute for Renewable Energy, Department of Chemistry, The University of Liverpool, L69 4ZF Liverpool, United Kingdom

Supporting Information

ABSTRACT: Chitosan/xanthan gum microcontainers with a core−shell structure formed due to chemical interactions between polysaccharide chains induced by ultrasonication are presented. Containers were prepared by sonication of water-immiscible (oil-like) liquids in the solution of polysaccharides. One-step fabrication of the container permanent shell is possible, because of the contribution of ultrasonically caused formation of hydrogen bonds and amide linkages. We synthesized containers in a wide size range from 350 nm to 7500 nm, varying in oil/water ratio. The microcontainers were modified with oppositely charged polyelectrolytes and microparticles, which could be used to impart the specified properties to the system. The biocide 4,5-dichloro-2-*n*-octyl-4-isothiazoline-3-one (DCOIT) was loaded into the proposed containers by utilizing its solution as an oil phase. The following incorporation of the DCOIT containers into the polymer coating demonstrated more sustained antimicrobial activity (~30%) of the biocide in the encapsulated state, compared to its non-encapsulated form.

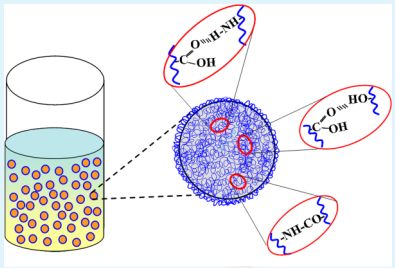

KEYWORDS: *microcontainer, hydrophobic bioactive agent, ultrasound, emulsification*

INTRODUCTION

Despite numerous methods that have been successfully applied for the fabrication of microscaled carriers filled by hydrophobic bioactive substances,[1] continuous efforts are made to develop new encapsulation techniques, because of the need to obtain a stable delivery system via a simple and economic procedure. In most cases, water-immiscible components are encapsulated via an emulsion route,[2] which requires additional stabilization of a colloidal system by different types of surfactants, surface-active polymers, proteins, polysaccharides, or their mixtures. To date, several techniques have been developed to produce emulsions, such as high-pressure homogenization, microfluidization, membrane contractor technique, ultrasonication, etc.[3−6] The last technique is most promising for the simultaneous encapsulation of prepared emulsion droplets, because of various sonochemical effects that accompany the ultrasonic comminution in a liquid−liquid system.

Ultrasound produces cavitations (the formation, growth, and collapse of cavitation bubbles), which is an underlying primary cause of sonochemical effects.[7] The extreme conditions inside a cavitation bubble (5000 K, 1000 atm) lead to various physical processes or/and chemical reactions creating spherical shells, which contain either gas or liquid in their inner cavity. In the case of the formation of microspheres under the influence of ultrasound, the cavitation bubble played a role of a quasi-stable template with unique physicochemical characteristics of the surface. The mechanism responsible for microcapsule formation is a combination of two processes: emulsification and cavitation.[1]

The microcapsules are fabricated in polymer solution layered over water-immiscible solvent by sonication in a shorter period than by the usual microencapsulation methods.[8,9] A sonochemical encapsulation process has no demand on special equipment and materials: only sonotrode is required. The ultrasonic emulsification occurs in the mixture of polymer solution and water-immiscible liquid, which contains bioactive agents to be encapsulated. Microcapsule shells composed of polymer are synthesized at the interface between oil and the polymer solution within a few minutes. Moreover, the one-step ultrasonically assisted encapsulation procedure is extremely effective in producing microspheres with high encapsulation efficacy.[10]

Suslick and co-workers were the first to demonstrate the successful application of high-intensity ultrasound to produce protein microspheres and fabricated by this sonochemical method microcontainers with shells made of proteins (bovine serum albumin, human serum albumin, hemoglobin, and myoglobin).[11,12] The mechanism of protein shell formation

Received: January 9, 2014
Accepted: April 8, 2014
Published: April 8, 2014

   dx.doi.org/10.1021/am406039r | ACS Appl. Mater. Interfaces 2014, 6, 6570−6578

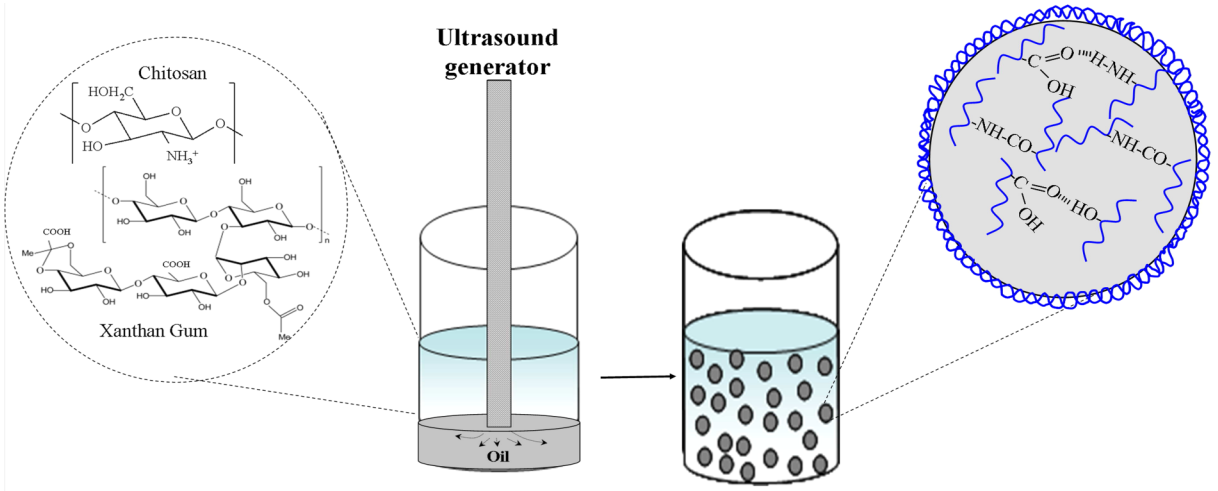

Figure 1. Schematic representation of the microcontainer formation.

was explained by effect on interaction of the free radicals generated during the sonication process on protein molecules leading to their cross-linking through disulfide bridges. Lately, Gedanken and co-workers synthesized protein microspheres from avidin and streptovidin, which do not possess sulfur-containing cysteine moieties.[13] In their opinion, hydrophobic interactions and thermal denaturation assist the sphere formation. Suslick et al. also obtained the polyglutamate spheres, which were stable over a wide range of pH values, because of hydrogen bonding networks.[14]

To date, several research groups followed this approach to fabricate various spheres/containers, utilizing different proteins or polymers with protein moieties, e.g., bovine serum albumin capsules were demonstrated in refs 15 and 16, capsules from polyglutamic acid were demonstrated in refs 14 and 17, α-amylase microspheres were demonstrated in ref 18, lysozyme microbubbles were demonstrated in ref 19, and containers based on gum arabic were demonstrated in ref 20. High biocompatibility and biodegradability of proteins as material for the containers' buildup can be considered as benefits for their potential application. On the other hand, relatively high costs of these substances, as well as their low long-term stability, significantly limit their universal use, especially in application fields other than the biomedical one.

Here, we present a new class of oil-filled microcontainers with core−shell morphology, which can be prepared in one-step procedure by applying a low-frequency ultrasonic treatment. The advantage of these microcapsules, compared to ones proposed earlier, is the chemical nature of their shells, which are composed exclusively of polysaccharides, chitosan, and xanthan gum, which stabilizes microcapsules in a broad pH range. The shell of the containers was composed of two polymers, which create a permanent structure of the system, because of the ultrasonically induced chemical interactions between them. The previously demonstrated containers were mostly fabricated based on the nonhuman protein types (such as bovine serum albumin), thus being quite allergenic. Therefore, the probability of getting an immune response to proteins is much higher than getting such a response to polysaccharides. On the other hand, human proteins are frequently very expensive,[21,22] making polysaccharides more attractive as shell components for the development of carriers for biomedical applications.

Chitosan possesses many useful biomedical properties, including biocompatibility, biodegradability, bioactivity, fungistatic nature, and a lack of both toxicity and allergenicity.[23] Therefore, it is widely used in numerous applications, ranging from pharmaceutical and cosmetic products to water treatment and plant protection.[24] Xanthan gum is also a fully biodegradable polymer stable over a broad pH range and exhibits several favorable rheological properties such as high at-rest or low-shear viscosity and high pseudo-plasticity.[25] It is widely used in various applications, such as the food, pharmaceuticals, and cosmetics industries.[26]

RESULTS AND DISCUSSION

Chitosan and xanthan gum, as a polycation and polyanion, respectively, can spontaneously form a polyelectrolyte complex. Prevention of a complex formation is an important precondition for the ultrasonically assisted microcontainer fabrication applying these two polymers. To avoid electrostatic interaction between the polysaccharides in the mixture, pH values of their solutions were adjusted to the acidic. The dissociation of D-glucuronic acid and pyruvic acid units, which determine[27] the character of xanthan gum as a weak acid, is completely suppressed within this pH range. In contrast, primary amine groups of chitosan[28] are protonated in the same pH range, providing its good solubility.

Figure 1 shows a scheme of the microcontainer fabrication. The mixture of chitosan and xanthan gum was layered with nonaqueous liquid and exposed to high-intensity ultrasonication. Cross-linking of both polysaccharides due to chemical interactions between their amino, hydroxyl, and carboxyl functional groups is induced by high energy ultrasound treatment. The production of highly reactive free radicals, such as $OH^{\bullet}$ and $H^{\bullet}$, during acoustic cavitation in water,[11] results in chemical reactions between functional groups located at the interface between a dispersed phase and a dispersion medium. It leads to the creation of a stable layer at the droplet surface and, subsequently, to the formation of permanent shells of microcontainers.

We applied the proposed method to fabricate the microcontainers loaded with different types of "oils", such as miglyol, soybean oil, hexane, cyclohexane, and toluene. The change of oil phase had no effect on the colloidal stability of the system, which evidences that the chemical nature of the oil used does

dx.doi.org/10.1021/am406039r | ACS Appl. Mater. Interfaces 2014, 6, 6570−6578

not influence the generation of free radicals upon sonication and also does not participate in the shell formation process.

We used Fourier transform infrared (FTIR) spectroscopy to investigate chemical transformations induced by the sonication of the polymer mixture. Figure 2 shows spectra of chitosan, xanthan gum, and their mixture extracted from the container shell in the range from 800 cm^{-1} to 1800 cm^{-1} (full spectra are given in the Supporting Information (SI)). The band observed at 1651 cm^{-1} (NH_2 deformation in primary amines) in the chitosan spectrum is shifted in the mixture spectrum to 1633 cm^{-1} (C═O stretch and NH_2 deformation in primary amides), while a peak at 1402 cm^{-1} in the xanthan gum spectrum (OH bending in carboxylic acids) vanishes completely in the spectrum of the mixture. This evidence demonstrates the amide linkage formation between functional groups of the polymers. In addition, the band at 1587 cm^{-1} in the chitosan spectrum that is assigned to NH_2 deformation is shifted in the mixture to a significantly lower wavenumber (1529 cm^{-1}), which indicates the participation of chitosan primary amino groups in the reaction between polymers induced by the ultrasonication. The spectrum of the polymer mixture extracted from the containers exhibits a new peak at 1493 cm^{-1} (amide II band), which reveals the formation of amide bonds. All of these results confirm the chemical reaction between chitosan $-NH_2$ groups and −COOH of acetate or pyruvate groups in xanthan gum molecules caused by the ultrasound treatment.

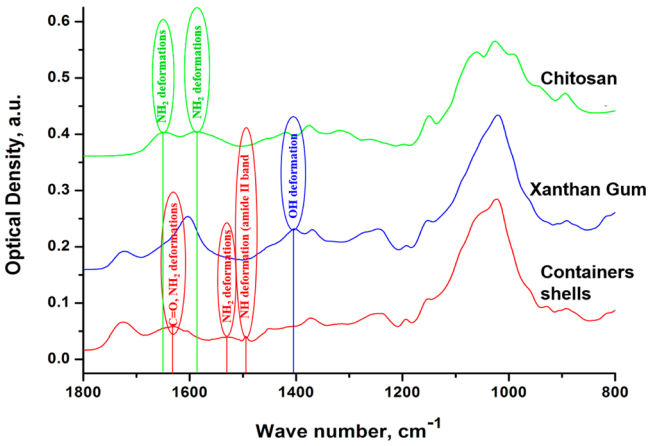

Figure 2. Fourier transform infrared (FTIR) investigations of the pristine chitosan, xanthan gum, and the polymer mixture treated with ultrasound (extracted from the microcontainers).

Changes in the FTIR spectrum of polysaccharide mixture registered after ultrasound-mediated microcontainer synthesis allow the assumption of the following mechanism of their formation. The acidic pH of the initial polymer solutions keeps xanthan gum in a nondissociated state and provides simultaneously a perfect solubility of chitosan. In the first step, the hydrogen bonds are formed between the polar groups (−COOH and $-NH_2$, −OH, and −COOH), maintaining a primary structure of the container shell. The second step consists of ultrasound-induced formation of amide linkages, which contribute to the final buildup of the permanent core−shell structure of the microcontainer.

By varying an oil/water ratio (from 1:300 to 1:1.5, respectively), we easily obtained the containers in a wide size range (from 350 ± 50 nm to 7500 ± 500 nm), whose morphology and structure were investigated by cryo-scanning electron microscopy (cryo-SEM) (see Figure 3), demonstrating well-separated containers with a narrow size distribution. The higher-magnification image (Figure 3C) of microcontainers with broken shells reveals their core/shell structure. The thin external polymer shell (Figure 3C) surrounds the inner container core. The estimated thickness of the shell is ∼7−10 nm, which, however, is robust enough to keep the microcontainers stable during storage at 4 °C for at least 6 months. The container size changed from 1160 ± 200 nm (PDI 0.417 ± 0.08) to 1250 ± 150 nm (PDI 0.504 ± 0.1) over this period of storage.

The container size steadily decreases as the water phase/oil phase ratio increases. Figure 4 demonstrates the dependence of

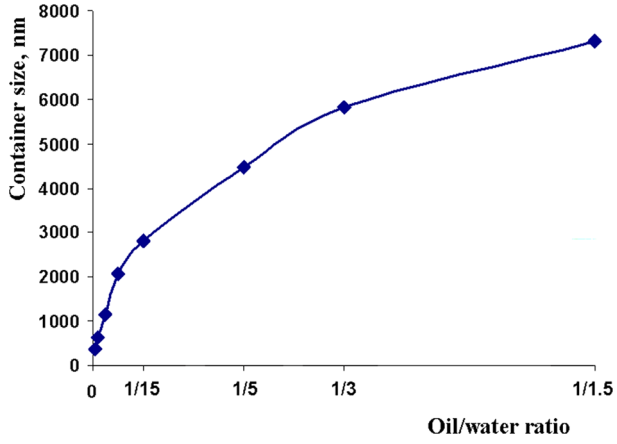

Figure 4. Dependence of the container size on the oil/water ratio. Each size value was averaged from five subsequent measurements from each of 20 runs.

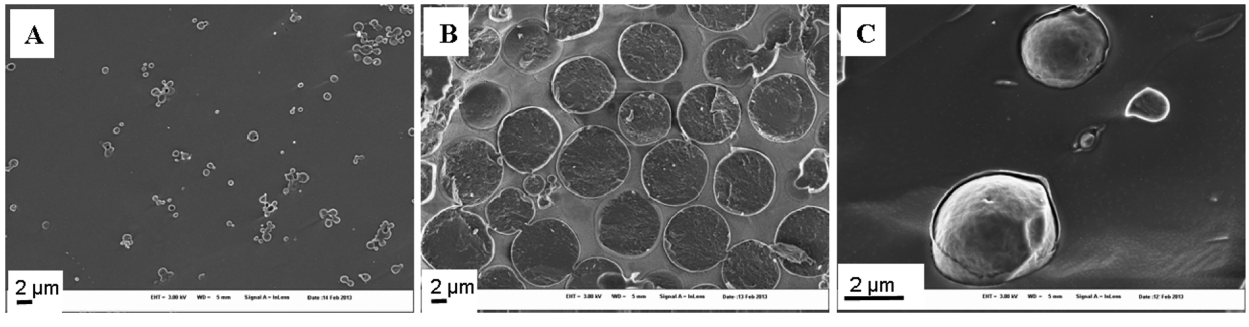

Figure 3. Cryo-scanning electron microscopy (cryo-SEM) observations of the microcontainers with different size: (A) 1160 nm (PDI = 0.417), oil/water ratio 1/60; (B) 7324 nm (PDI = 0.146), oil/water ratio 1/1.5; and (C) containers with broken shells.

dx.doi.org/10.1021/am406039r | ACS Appl. Mater. Interfaces 2014, 6, 6570−6578

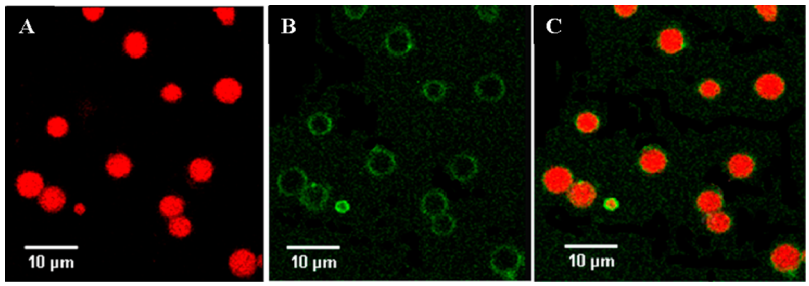

Figure 5. CLSM observation of the system modified by PAH-FITC (panel C), red emission from Nile Red (panel A), green emission from PAH-FITC (panel B).

the container size on the oil/water ratio. This dependence can be explained by changing the overall emulsion viscosity.[29,30] Drops of the emulsion that are placed in a turbulent continuous phase (during ultrasonication) break upon the action of viscous or inertial stress acting on the drop surface. The regime of emulsification in turbulent flow can be changed from inertial to viscous one by the increase of the oil volume fraction, which leads to the change of the overall emulsion viscosity.[30] In the opposite case of the decreasing viscosity, the drop size in the emulsion is strongly reduced due to transition from the viscous to the inertial regime of the emulsification.[29] The soybean oil loaded microcontainers of 5.2 μm (PDI = 0.389) size were used for further characterization.

Polydispersities of all obtained emulsions were quite moderate (PDI $\leq$ 0.5) independent of the oil/water ratio. This observation allows the assumption that not only mechanical forces but also some additional factors such as enthalpy and entropy changes during the emulsification can contribute to the monodispersity of final systems. On the one hand, increase of the total area of the interface between oil and water phases in the emulsion should enhance the system enthalpy, making the emulsion formation energetically unfavorable. On the other hand, the strong simultaneous increase of the entropy in the system can be considered as a significant benefit of the emulsification. The interplay of both these contributions (enthalpic and entropic) to the changes in the free Gibbs energy of the system lead to the most favorable and, therefore, stable state where the change in the Gibbs free energy of the system has a minimal positive value (because, strictly speaking, such systems, as conventional emulsions, are thermodynamically instable). This general consideration is consistent with the dependence of emulsion droplet size on the oil/water ratio: The lower this ratio, the smaller the droplets and the higher their total surface area, but also the greater their number and the corresponding increase of the entropy in the system. In the case of the high oil/water ratio, the increases in both the enthalpic and entropic contributions upon emulsification are moderate, because of larger droplets (i.e., of weaker increase of droplets surface area and disorder in the system, correspondingly). Consequently, an almost-monodisperse emulsion but with larger droplets can be produced.

The images in Figure 5 show confocal laser scanning microscopy (CLSM) observation of the containers filled with solution of a fluorescent dye Nile Red in soybean oil, which surface was labeled by the deposition of PAH-FITC. The microphotographs demonstrate a presence of green fluorescence from the shell (adsorbed PAH-FITC, Figure 5B) of the microcontainers with the red inner core (Figure 5A). Figure 5C confirms the core/shell morphology of obtained microcontainers as derived above on the basis of SEM. The measurements of the zeta-potential showed changes of the surface charge of microcontainers from −50 mV (initial containers) to +52 mV upon modification with cationic PAH-FITC. On the other hand, polymer adsorption has no influence on the system stability. The microcontainers also remained non-aggregated and well-dispersed after their surface modification. Moreover, an interfacial attachment of negatively charged SiO_2 nanoparticles to the outer surface of PAH-coated container shell demonstrates further possibilities of container modification.

The main advantage of the proposed approach for the container preparation is the lack of use of environmentally harmful volatile organic compounds (VOCs) or metal-based catalysts, which are required for most common container fabrication techniques, such as spray-drying, polyaddition, etc.

An excellent demonstration of the high practical relevance of developed containers is the successful encapsulation of the novel green biocide DCOIT for further applications in aqueous antifouling coatings. DCOIT is a broad spectrum biocide with very good biodegradability and was recently recommended as an environmentally friendly biocide for use in many different applications: wood preservation, plastics, sealants, marine antifouling, and indoor coatings.[31] This biocide has low water solubility and, therefore, good leach resistance from the dried coatings contributing to its very sustained protection performance. However, the same peculiarity restricts the use of DCOIT to only solvent-based coating formulations: it is almost impossible to distribute this substance homogeneously in an aqueous coating formulation, finally leading to the violation of the coating integrity and to the subsequent loss of barrier properties of these coatings after curing. On the other hand, because of steadily raising environmental regulations limiting or even banning the use of VOC in many industrial fields, the development and application of water-based coating formulations became increasingly more necessary. Therefore, successful implementation of highly hydrophobic DCOIT in aqueous coating formulations will imply the development of a new generation of very efficient and simultaneously ecofriendly antifouling paints.

Another advantage of the DCOIT-loaded containers is the microbial triggering of their opening (see Figure 6A). Stimuli responsive regulation of the biocide release can be realized, because of the microbial decomposition of the container shell:[32,33] The higher the growth rate of the microorganisms population, the stronger the shell deterioration, providing the active bacteriostatic and/or fungistatic feedback. The released biocide inhibits growth of the microorganisms on the surface of coatings with the embedded containers, thereby imparting to them specific antimicrobial functionalities, which can be activated upon demand.

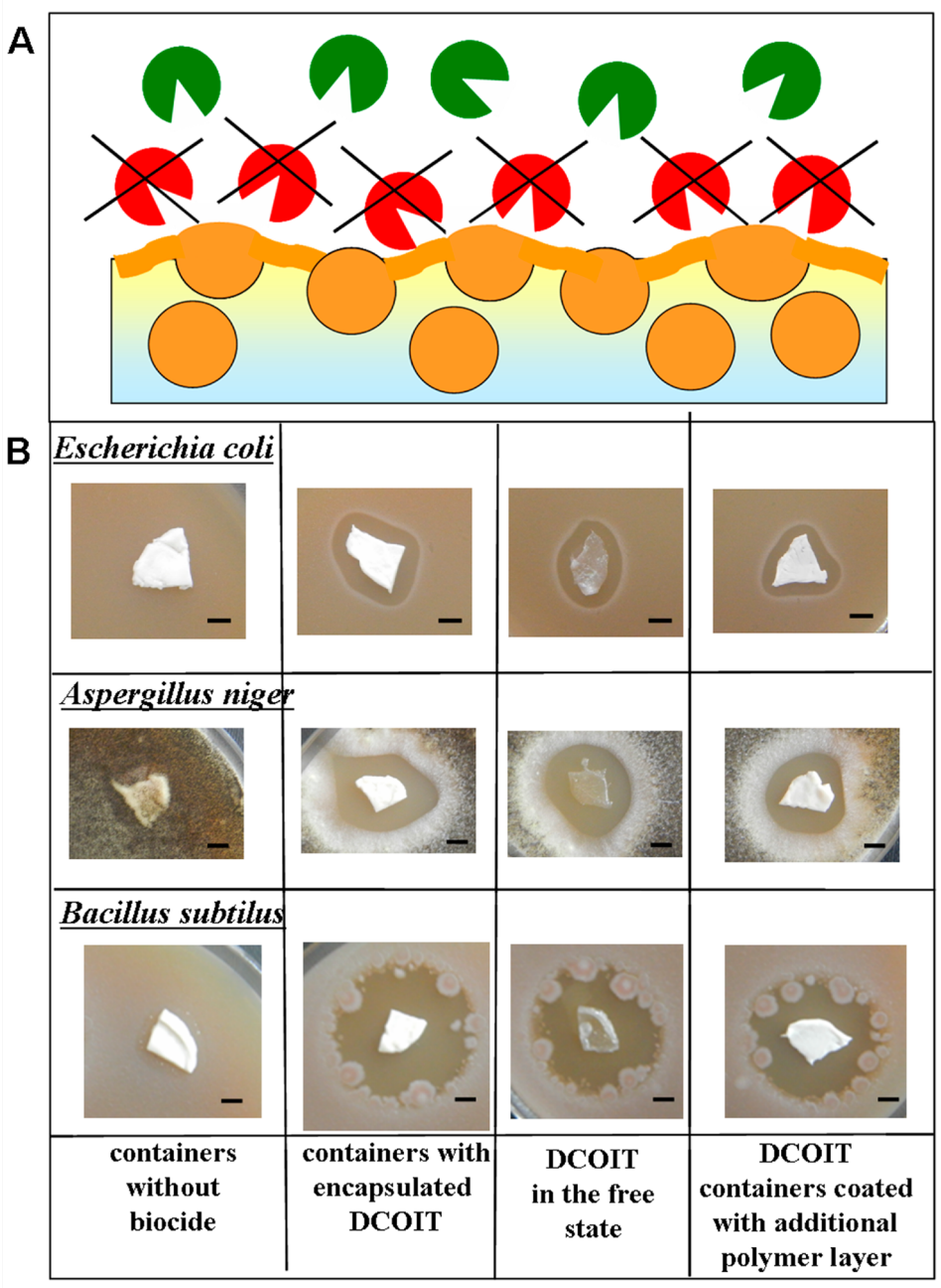

Figure 6. (A) Scheme of microbial triggering of the container opening: microbial decomposition of the container shell leads to release of encapsulated biocide followed by growth inhibition of the microorganisms. Bacteriostatic and fungistatic activities of both encapsulated DCOIT and DCOIT in the free state against Gram-positive bacteria *Bacillus subtilus* ATCC 6633, Gram-negative bacteria *Escherichia coli* ATCC 25922, and mycelial fungus Aspergillus niger ATCC 16404 in Ca-alginate polymer film after 24 h of incubation (in the case of bacteria) and 48 h of incubation (in the case of fungus) (scale bar is 5 mm).

Comparative agar diffusion tests for the evaluation of biocidic efficiency of the encapsulated DCOIT against three representative microorganisms—Gram-positive bacteria *Bacillus subtilus* ATCC 6633, Gram-negative bacteria *Escherichia coli* ATCC 25922, and mycelial fungus *Aspergillus niger* ATCC 16404—were performed (see Figure 6B).[34] We examined two samples with encapsulated DCOIT: the initial microcontainers with biocide and the DCOIT containers coated with an additional layer of PAH. Two supplementary samples were prepared for control: a sample with containers that do not contain biocide and a sample with free distributed DCOIT. All samples were placed on the surface of agar plate previously inoculated with the microorganisms to be tested. The plates were incubated at 37 °C for 24 h (in the case of bacteria) or at 28 °C for 48 h (in the case of fungus).

Figure 6B demonstrates the presence of inhibition zones of microbial growth (clear rings) around the sample with the biocide in a freely dispersed state, around the sample with the encapsulated DCOIT, and around the sample with the biocide containers modified with the PAH. The obtained results indicate a good diffusion of the biocide from the containers. We found a double zone of inhibition in the case of *Aspergillus niger*: the total zone of growth inhibition, followed by the zone of sporulation inhibition. There was no inhibition zone around

dx.doi.org/10.1021/am406039r | *ACS Appl. Mater. Interfaces* 2014, 6, 6570−6578

the sample without biocide (negative control), which evidences the nontoxicity of the container's material for the microorganisms.

The mode of DCOIT action is very fast and utilizes a two-step mechanism involving rapid growth inhibition, leading to a loss of viability.[35] In the case of the film with the embedded containers, the greatest inhibition effect was observed against *Bacillus subtilus* with a zone of inhibition of 26 mm, followed by *Aspergillus niger* with a zone of inhibition of 21.5 mm and *Escherichia coli* with a zone of inhibition of 16 mm. We found slightly delayed DCOIT inhibition action in the case of the film with free distributed DCOIT (*Bacillus subtilus,* 24.2 mm; *Aspergillus niger*, 20 mm; *Escherichia coli*, 14.5 mm). The films with incorporated coated containers showed more sustained inhibition activity, compared to previous samples: 23.2 mm of the inhibition zone against *Bacillus subtilus*, 17.7 mm in the case of *Aspergillus niger*, and 14.6 mm against *Escherichia coli.* The results demonstrate that an additional coating with PAH decelerate the DCOIT diffusion from the film and, thus, could make its bacteriostatic and fungistatic activities essentially more sustained.

To compare a diffusion character of encapsulated DCOIT and DCOIT in the free state, we examined the activity of the samples against *Escherichia coli.* The encapsulated biocide showed an equal activity after 24 h of incubation comparing to the same concentration of the freely dispersed DCOIT (10 μg/mL). The results after 48 h of incubation demonstrate more sustained (~30%) activity of DCOIT microcontainers, indicating their prolonged performance in the coatings: 11.5 mm of inhibition zone for freely dispersed DCOIT versus 14 mm of inhibition zone for the encapsulated DCOIT (see the SI).

At first glance, the biocide incorporated in the Ca-alginate matrix in the free state should diffuse faster than the encapsulated one. However, in reality, one must additionally recognize (i) the strong hydrophobicity of DCOIT and (ii) its significant instability against chemical degradation. The first factor leads to the aggregation of the DCOIT powder in the hydrophilic Ca-alginate matrix and, as a consequence, also leads to the strong decrease of the total surface area of the DCOIT particles incorporated in the polymer film. In contrast, the hydrophilicity of polysaccharide shells of DCOIT-filled microcontainers provides essentially homogeneous distribution of these in the Ca-alginate matrix, resulting in the much-higher total surface area of all incorporated microcontainers filled with the same amount of DCOIT. Therefore, even in the case of lower diffusivity of the encapsulated DCOIT from the containers, the high total cross-section area of all containers participating in the release leads to the diffusion flux compatible or higher than one for the free incorporated biocide.

Moreover, the fast degradation of DCOIT in the free state contributes to the less-sustained diffusion flux of the biocide, especially in the long-term perspective. Thus, the inhibition zone for the microorganisms growth in the case of the encapsulated (i.e., protected) DCOIT becomes, after 48 h of exposition time, broader than that for the biocide incorporated in the free state. It is well-known from the literature that DCOIT rapidly degrades in marine and freshwater environments (half-life times of <1 h and <3 h, respectively) and bioaccumulation of parent molecule is very low.[36,37] Therefore, 48 h of incubation could leads to the considerable biocide decomposition incorporated in the matrix in the free state, while the encapsulation of the substance into the containers protects the biocide from degradation and correspondingly extends the period of its antimicrobial activity. These results are in agreement with ref 38, where the authors demonstrated that the degradation of DCOIT included in the paint particles led to an increase in the half-life, up to 10 days, compared to less than 1 day for DCOIT in free form.

In addition, delayed DCOIT antimicrobial activity after 48 h of incubation could be explained in view of mechanism of the biocide action. The mode of action of DCOIT is very fast. The biocide rapidly associated with microbial cells and inhibited cellular activity within minutes.[35]

To examine the influence of the polymer coating on the DCOIT release level, we investigated the release rate of biocide for unmodified containers and containers coated with an additional polyelectrolyte (PAH). The release occurring is based on the diffusion of biocide from the containers confined in a dialysis tubing to an external aqueous phase. We observed the influence of the container modification on the rate of the DCOIT release. In the first hours, the polyelectrolyte-coated containers showed the release of the biocide, which was slower by a factor of 2, compared to unmodified ones (see Figure 7).

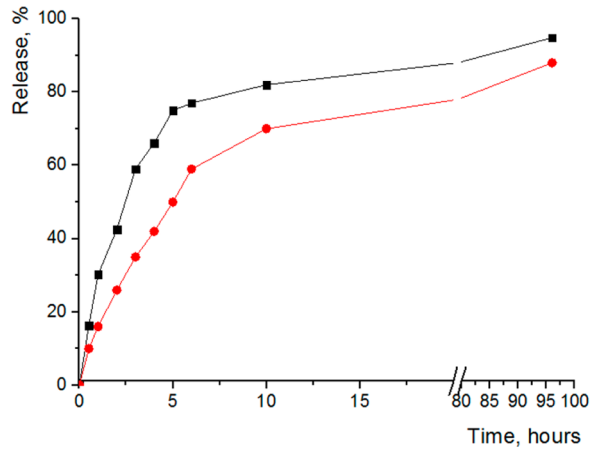

Figure 7. Release profile of DCOIT from (■) the initial containers and (●) the containers modified with a polymer layer.

Approximately 82% of DCOIT was released within 10 h in the case of initial containers, while modified containers showed that only 70% of the biocide was released within the same period. The modification of the container surface imparts prolonged release properties to the system, presenting more sustained release of the encapsulated biocide.

DCOIT is a hydrophobic compound with very low water solubility. We performed the release experiment in sodium chloride solution (pH 7.5), maintaining the sink conditions for DCOIT. The more-sustained release of DCOIT from the coated containers could be interpreted due to increase of the container shell hydrophilicity, as the result of an additional polyelectrolyte layer (PAH) adsorption. Upon release from the containers, hydrophobic DCOIT must penetrate through hydrophilic containers shells. Therefore, the increase of the diffusion path of DCOIT molecules within container shells should lead to the slower release of the biocide. Moreover, hydrophobic−hydrophobic interactions between backbone chain of PAH and octyl chain of DCOIT can also contribute to further slowing of the release.

These results are in a good agreement with previous observations, where tests of bacteriostatic and fungistatic

activities demonstrated a diminution of the growth inhibition zone of microorganisms around the containers modified by the additional polymer layer, compared to that of the initial containers (Figure 6B).

EXPERIMENTAL SECTION

Materials. Chitosan (20-300 cP), xanthan gum (from *Xanthomonas campestris*), poly(allylamine hydrochloride) (MW 70000), sodium alginate (medium viscosity), fluorescein isothiocyanate (FITC), soybean oil, hexane, cyclohexane, and toluene were supplied from Sigma–Aldrich (Germany). 4,5-Dichloro-2-*n*-octyl-4-isothiazoline-3-one (DCOIT) was purchased from Chemos GmbH (Germany). Miglyol 812 Neutral Oil (a mixture of medium chain caprylic/capric triglycerides, MCT) was provided by Sasol Germany GmbH (Witten, Germany), Batch No. 080708. All materials were used without further purification.

Synthesis of Container. Equal volumes of chitosan and xanthan gum solutions (0.25 wt %, pH 2) were mixed, then layered with nonaqueous liquid and exposed to high-intensity ultrasound, using a 7-mm-diameter titanium sonotrode (56 W cm^{-2}, 20 kHz, 5 min) (Ultrasonic Processor UP400S, Hielscher Ultrasonics GmbH, Germany). The freshly prepared microcontainers were centrifuged (1.677*g*, 10 min), washed with water, and then incorporated into a Ca-alginate film or modified with poly(allylamine hydrochloride) (PAH)) for fluorescent labelling and embedded into the polymer film. Sodium alginate was used here as a model polymer, which easily forms the film by cross-linking with Ca^{2+} ions. Namely, a mixture of 1 wt % sodium alginate solution and the containers was poured onto a cellulose filter (Millipore) saturated with 2 wt % $CaCl_2$ solution and covered by the same filter for 15 min. The cross-linked film was washed with physiological solution and kept in the refrigerator. In order to modify the container surface, they were incubated in PAH-FITC solution (1 mL, 2 mg mL^{-1}, 0.5M NaCl) under shaking (Vortex-genie 2, Scientific Industries, Inc., USA) at room temperature (RT) for 15 min. After the incubation, the containers were isolated by centrifugation (1.677*g*, 10 min) and washed three times with water to remove the polyelectrolyte excess.

Container Characterization. *Fourier Transform Infrared (FTIR) Measurements.* Fourier transform infrared (FTIR) measurements were performed at RT on KBr pellets with a Bruker Hyperion 2000 IR spectrometer. The pellets were fabricated from a mixture of polymer powder and potassium bromide, using a manual pellet press (Specac, Orpington, U.K.), and mounted on a QuickLock base plate. Spectra in the range from 400 cm^{-1} to 4000 cm^{-1} were recorded with 2 cm^{-1} resolution in the transmission mode, using a DTGS detector. For FTIR measurements, the microcontainers loaded with hexane were mechanically milled and to pounded with a pestle. The polymers were dried in a desiccator for 3 h, and the powder was investigated.

Confocal Observations (CLSM). Confocal observations (CLSM) were carried out using a Leica TCS SP confocal scanning system (Leica, Germany) equipped with a 100× oil immersion objective (numerical aperture (NA), 1.4).

Cryo-Scanning Electron Microscopy (cryo-SEM). The morphology of the containers was studied using cryo-scanning electron microscopy (cryo-SEM). Each sample was frozen by plunging it into a nitrogen slush at atmospheric pressure. The samples were freeze-fractured at −150°C, etched for 60 s at −98°C, sputtered with platinum in the GATAN Alto 2500 Cryo preparation chamber, and then transferred into the cryo-SEM system.

Zeta Potential and Container Size. The zeta potential and container size were measured by a Zeta Sizer Nano (Malvern Instruments, U.K.). Each zeta potential value was averaged from three subsequent measurement series (15 runs each), and the size value was averaged from five subsequent measurements (20 runs each).

Antimicrobial Activity Test. *Preparation of the Containers.* Five milliliters (5 mL) of chitosan (0.25 wt %, pH 2) and 5 mL of xanthan gum (0.25 wt %, pH 2) were mixed, then layered with 500 μL of preheated up 45 °C DCOIT and exposed to high-intensity ultrasound, using a 7-mm-diameter titanium sonotrode (56 W cm^{-2}, 20 kHz, 5 min) (Ultrasonic Processor UP400S, Hielscher Ultrasonics GmbH, Germany). The freshly prepared microcontainers were centrifuged (1.677*g*, 10 min), washed with water, and then incorporated into a Ca-alginate film or modified with PAH and embedded into the polymer film.

Preparation of Polymer Films. A mixture of 500 μL of 1 wt % sodium alginate solution and the containers was poured onto a cellulose filter (Millipore) saturated with 2 wt % $CaCl_2$ solution and covered by the same filter for 15 min. The cross-linked film was washed with physiological solution and kept in the refrigerator.

The following samples were prepared:

(1) Ca-alginate film containing 50 μL of the containers loaded with soybean oil (negative control);
(2) Ca-alginate film containing 50 μL of the containers loaded with DCOIT (42.5 μg of DCOIT);
(3) Ca-alginate film containing 42.5 μg of DCOIT (positive control); and
(4) Ca-alginate film containing 50 μL of the DCOIT containers coated with PAH (42.5 μg of DCOIT).

Bacteriostatic and fungistatic activities of the samples were evaluated by comparative agar diffusion tests against three representative microorganisms: Gram-positive bacteria *Bacillus subtilus* ATCC 6633, Gram-negative bacteria *Escherichia coli* ATCC 25922, and mycelial fungus *Aspergillus niger* ATCC 16404. All samples were placed on the surface of an agar plate previously inoculated with the microorganisms to be tested. The plates were incubated at 37 °C for 24 h (in the case of bacteria) or at 28 °C for 48 h (in the case of fungus). Antimicrobial activity was assessed as inhibition zones of the growth of microorganisms around the samples.

Biocide Release. DCOIT release profile was investigated using a dialysis method. Namely, 100 μL of encapsulated DCOIT were resuspended in 5 mL of 0.5N NaCl solution and placed in a dialysis bag (Pur-A-Lyzer Mega 1000 Dialysis Kit Manual, PURG 10020, Sigma–Aldrich Labware, Germany). The dialysis kit was placed in sodium chloride release medium (50 mL). The study was performed in an incubator shaker at 300 rpm at RT (BioShaker XP, Q.Instrument GmbH, Germany). At various time points, the release medium was completely replaced with fresh release medium and analyzed by UV-vis spectroscopy at 213 nm. The sink conditions were calculated based on DCOIT solubility, DCOIT amount contained in the containers, and total volume of release medium, and were maintained throughout the entire experimental time. Quantity of the released biocide was calculated and presented finally as a percentage (%) of its total entrapped amount.

CONCLUSIONS

In conclusion, we have proposed a new type of chitosan/xanthan gum microcontainer that has been fabricated via the simple one-step ultrasound treatment. The used shell components—polysaccharides, chitosan, and xanthan gum—are biocompatible, biodegradable, and lack allergenicity. These containers can be further modified upon demand with oppositely charged polyelectrolytes and/or particles. The subsequent successful embedding of containers with the encapsulated biocide DCOIT into the polymer coating showed the maintenance of the antimicrobial activity of the biocide in the encapsulated state, together with the more sustained character of coating performance, opening wide perspectives for the future applications of these containers in various types of functional coatings.

ASSOCIATED CONTENT

Supporting Information

FTIR spectra and antimicrobial activity test. This material is available free of charge via the Internet at http://pubs.acs.org.

AUTHOR INFORMATION

Corresponding Author

*E-mail: borodina@crys.ras.ru.

Author Contributions

The manuscript was written through contributions of all authors. All authors have given approval to the final version of the manuscript.

Notes

The authors declare no competing financial interest.

ACKNOWLEDGMENTS

This work was supported by the RFBR 12-03-93939-G8 project and the NANOMAR "Nanocontainer-Based Active Coatings for Maritime Applications" project. D.G. gratefully acknowledges the financial support from the European G8 project, "Multiscale smart coatings with sustained anticorrosive action—smart coat". The authors would like to thank Olga A. Galatenko and Larisa P. Terekhova for the help with the microbiological experiments.

REFERENCES

(1) Shchukina, E. M.; Shchukin, D. G. LbL Coated Microcapsules for Delivering Lipid-Based Drugs. *Adv. Drug Delivery Rev.* **2011**, *63*, 837−846.

(2) Grigoriev, D. O.; Haase, M. F.; Fandrich, N.; Latnikova, A.; Shchukin, D. G. Emulsion Route in Fabrication of Micro and Nanocontainers for Biomimetic Self-Healing and Self-Protecting Functional Coatings. *Bioinspired, Biomimetic Nanobiomater.* **2012**, *1* (BBN2), 101−116.

(3) Shchukina, E. M.; Shchukin, D. G. Layer-by-Layer Coated Emulsion Microparticles as Storage and Delivery Tool. *Curr. Opin. Colloid Interface Sci.* **2012**, *17*, 281−289.

(4) Li, G. L.; Möhwald, H.; Shchukin, D. G. Precipitation Polymerization for Fabrication of Complex Core−Shell Hybrid Particles and Hollow Structures. *Chem. Soc. Rev.* **2013**, *42*, 3628−3646.

(5) Grigoriev, D. O.; Miller, R. Mono- and Multilayer Covered Drops as Carriers. *Curr. Opin. Colloid Interface Sci.* **2009**, *14*, 48−59.

(6) Agarwal, A.; Lvov, Y.; Sawant, R.; Torchilin, V. Stable Nanocolloids of Poorly Soluble Drugs With High Drug Content Prepared Using the Combination of Sonication and LbL Technology. *J. Controlled Release* **2008**, *128*, 255−260.

(7) Leighton, T. G. *The Acoustic Bubble*; Academic Press Limited: London, 1994.

(8) Deasy, P. B. *Microencapsulation and Related Drug Processes (Drug and Pharmaceutical Sciences)*; Marcel Dekker: New York, 1984.

(9) Donbrow, M. *Microcapsules and Nanocapsules in Medicine and Pharmacy*; CRC Press: Boca Raton, FL, 1991.

(10) Webb, A. G.; Wong, M.; Kolbeck, K. J.; Magin, R. L.; Wilmes, L. J.; Suslick, K. S. Sonochemically Produced Fluorocarbon Microspheres: A New Class of Magnetic Resonance Imaging Agent. *Magn. Reson. Imaging* **1996**, *6*, 675−683.

(11) Suslick, K. S.; Grinstaff, M. W. Protein Microencapsulation of Nonaqueous Liquids. *J. Am. Chem. Soc.* **1990**, *112*, 7807−7809.

(12) Wong, M.; Suslick, K. S. Sonochemically Produced Hemoglobin Microbubbles. *MRS Symp. Proc.* **1995**, *372*, 89−94.

(13) Avivi, S.; Gedanken, A. S−S bonds are not required for the Sonochemical Formation of Proteinaceous Microspheres: The case of Streptavidin. *Biochem. J.* **2002**, *366*, 705−707.

(14) Dibbern, E. M.; Toublan, F. J.-J.; Suslick, K. S. Formation and Characterization of Polyglutamate Core−Shell Microspheres. *J. Am. Chem. Soc.* **2006**, *128*, 6540−6541.

(15) Tzhayik, O.; Cavaco-Paulo, A.; Gedanken, A. Fragrance Release Profile from Sonochemically Prepared Protein Microsphere Containers. *Ultrason. Sonochem.* **2012**, *19* (4), 858−863.

(16) Makino, K.; Mizorogi, T.; Ando, S.; Tsukamoto, T.; Ohshima, H. Sonochemically Prepared Bovine Serum Albumin Microcapsules: Factors Affecting the Size Distribution and the Microencapsulation Yield. *Colloids Surf., B* **2001**, *22* (3), 251−255.

(17) Teng, X.; Shchukin, D. G.; Möhwald, H. Encapsulation of Water-Immiscible Solvents in Polyglutamate/Polyelectrolyte Nanocontainers. *Adv. Funct. Mater.* **2007**, *17*, 1273−1278.

(18) Avivi, S.; Gedanken, A. Are Sonochemically Prepared Alpha-Amylase Protein Microspheres Biologically Active? *Ultrason. Sonochem.* **2007**, *14*, 1−5.

(19) Cavalieri, F.; Ashokkumar, M.; Grieser, F.; Caruso, F. Ultrasonic Synthesis of Stable, Functional Lysozyme Microbubbles. *Langmuir* **2008**, *24*, 10078−10083.

(20) Borodina, T.; Grigoriev, D.; Markvicheva, E.; Mohwald, H.; Shchukin, D. Vitamin E Microspheres Embedded Within a Biocompatible Film for Planar Delivery. *Adv. Eng. Mater.* **2011**, *13* (3), B123−B130.

(21) Houdebine, L.-M. Production of Pharmaceutical Proteins by Transgenic Animals. *Comp. Immunol. Microbiol. Infect. Dis.* **2009**, *32* (12), 107−121.

(22) Mihaela, M. E; Sardiu, E.; Cai, Y.; Jin, J.; Swanson, S. K.; Conaway, R. C.; Conaway, J. W.; Florens, L.; Washburn, M. P. Probabilistic Assembly of Human Protein Interaction Networks from Label-free Quantitative Proteomics. *Proc. Natl. Acad. Sci. U.S.A.* **2007**, *105* (5), 1454−1459.

(23) Şenel, S.; McClure, S. J. Potential Applications of Chitosan in Veterinary Medicine. *Adv. Drug Delivery Rev.* **2004**, *56*, 1467−1480.

(24) Dutta, P. K.; Dutta, J.; Tripathi, V. S. Chitin and Chitosan: Chemistry, Properties and Applications. *J. Sci. Ind. Res.* **2004**, *63*, 20−31.

(25) Katzbauer, B. Properties and Applications of Xanthan Gum. *Polym. Degrad. Stab.* **1998**, *59*, 81−84.

(26) Sanderson, G. R. Application of Xanthan Gum. *Br. Polym. J.* **1981**, *13*, 71−77.

(27) Jansson, P. E.; Kenne, L.; Lindberg, B. Structure of Extracellular Polysaccharide from Xanthomonas Campestris. *Carbohydr. Res.* **1975**, *45*, 275−82.

(28) Aranaz, I.; Harris, R.; Heras, A. Chitosan Amphiphilic Derivatives: Chemistry and Applications. *Curr. Org. Chem.* **2010**, *14*, 308−330.

(29) Tcholakova, S.; Lesov, I.; Golemanov, K.; Denkov, N. D.; Judat, S.; Engel, R.; Danner, T. Efficient Emulsification of Viscous Oils at High Drop Volume Fraction. *Langmuir* **2011**, *27*, 14783−14796.

(30) Vankova, N. S.; Denkov, N. D.; Ivanov, I. B.; Vulchev, V.; Danner, T. Emulsification in Turbulent Flow 1. Mean and Maximum Drop Diameters in Inertial and Viscous Regimes. *J. Colloid Interface Sci.* **2007**, *312*, 363−380.

(31) Document II-A: Study Summaries—Dossier for Active Substance 4,5-Dichloro-2-octyl-4-isothiazolin-3-one (DCOIT). In *Product Type 10: Masonry Preservatives, Reporter Member State (RMS): Norway*; Rohm and Haas Company: Philadelphia, PA, 2010; pp 1−18.

(32) Gooday, G.W. Physiology of Microbial Degradation of Chitin and Chitosan. *Biodegradation* **1990**, *1* (2), 177−190.

(33) Cadmus, M. C.; Slodki, M. E. Bacterial Degradation of Xanthan Gum. In *Industrial Polysaccharides. Genetic Engineering, Structure/Property Relations and Applications*; Progress in Biotechnology 3; Elsevier Science Publishers: Amsterdam, Oxford, New York, Tokyo, 1987.

(34) National Committee for Clinical Laboratory Standards. *Reference method for broth dilution antifungal susceptibility testing of conidium-forming filamentous fungi*, Approved standard M38-A. National Committee for Clinical Laboratory Standards (NCCLS) (now Clinical and Laboratory Standards Institute (CLSI)): Wayne, PA, 2002.

(35) Williams, T. M. The Mechanism of Action of Isothiazolone Biocide. *PowerPlant Chem.* **2007**, *9* (1), 14−22.

(36) Jacobson, A. H.; Willingham, G. L. Sea-Nine Antifoulant: An Environmentally Acceptable Alternative to Organotin Antifoulants. *Sci. Total Environ.* **2000**, *258* (1-2), 103−110.

(37) Thomas, K. V.; McHugh, M.; Waldock, M. Antifouling Paint Booster Biocides in UK Coastal Waters: Inputs, Occurrence and Environmental Fate. *Sci. Total Environ.* **2002**, *293* (1-3), 117−127.
(38) Thomas, K. V.; McHugh, M.; Hilton, M.; Waldock, M. Increased Persistence of Antifouling Paint Biocides when Associated with Paint Particles. *Environ. Pollut.* **2003**, *123* (1), 153−161.